Published in final edited form as:

Xie, W. J., Cha, S., Ohto, T., Mizukami, W., Mao, Y., Wagner, M., et al. (2018). Large Hydrogen-Bond Mismatch between TMAO and Urea Promotes Their Hydrophobic Association. Chem, 4(11), 2615-2627. doi:10.1016/j.chempr.2018.08.020.

Link to formal publication: 10.1016/j.chempr.2018.08.020

Large Hydrogen-Bond Mismatch between TMAO and Urea Promotes Their Hydrophobic Association

Wen JunXie, Seoncheol Cha, Tatsuhiko Ohto, Wataru Mizukami, Yuezhi Mao, Manfred Wagner, Mischa Bonn, Johannes Hunger, Yuki Nagata

Large Hydrogen Bond Mismatch between TMAO and Urea Promotes Their Hydrophobic Association

Wen Jun Xie,[1,2,†] Seoncheol Cha,[1] Tatsuhiko Ohto,[3] Wataru Mizukami,[4] Yuezhi Mao,[5] Manfred Wagner,[1] Mischa Bonn,[1,6,*] Johannes Hunger,[1,*] and Yuki Nagata[1,7,*]

[1] Max Planck Institute for Polymer Research, Ackermannweg 10, D-55128, Mainz, Germany

[2] College of Chemistry and Molecular Engineering, Peking University, Beijing 100871, China

[3] Graduate School of Engineering Science, Osaka University, 1-3 Machikaneyama, Toyonaka, Osaka 560-8531, Japan

[4] Department of Energy and Material Sciences, Faculty of Engineering Sciences, Kyushu University, 6-1 Kasuga-Park, Fukuoka, Japan

[5] Kenneth S. Pitzer Center for Theoretical Chemistry, Department of Chemistry, University of California at Berkeley, Berkeley, California 94720, USA

[6] Lead Contact

[7] Department of Theoretical and Computational Molecular Science, Institute for Molecular Science, Myodaiji, Okazaki, Aichi 444-8585, Japan

[†]Present address: Department of Chemistry, Massachusetts Institute of Technology, 77 Massachusetts Ave., Cambridge, Massachusetts 02139, USA

*Correspondence: nagata@mpip-mainz.mpg.de, hunger@mpip-mainz.mpg.de, bonn@mpip-mainz.mpg.de

SUMMARY

TMAO and urea are both osmolytes found in many marine animals, yet show opposite effects in (de-)stabilizing proteins. Gaining molecular-level insights into the TMAO-urea interaction in aqueous solution is a key step to elucidate their biological roles. Here, combined *ab initio* molecular dynamics simulations, polarization-resolved femtosecond infrared pump-probe spectroscopy, and nuclear magnetic resonance spectroscopy reveal that the hydrophobic interaction between TMAO and urea is favorable compared with the hydrogen-bonding interaction. The association of the hydrophobic methyl group of TMAO with urea is driven by the large mismatch between the strong TMAO-water hydrogen-bond and the weak urea-water hydrogen-bond. Our observations provide a rationale for the counteraction of osmotic pressure due to urea by TMAO.

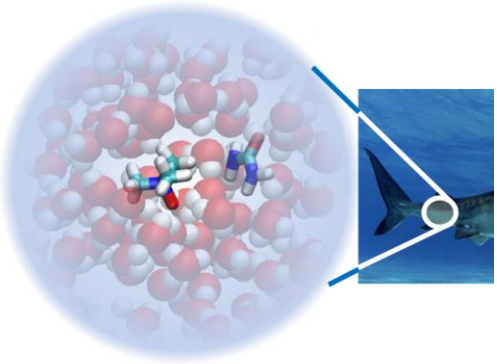

INTRODUCTION

Trimethylamine *N*-oxide (TMAO) and urea are both osmolytes, which allow living cells to adjust their osmotic pressure; with high concentrations of both urea and TMAO, marine animals can keep the osmotic pressure comparable to that of seawater.[1] Intriguingly, the effects of these osmolytes on protein structures are opposite; TMAO stabilizes the secondary structure of proteins,[2, 3] and can efficiently counteract protein denaturation due to urea, often at an approximate molecular ratio of 1:2 (TMAO:urea).[4, 5] The molecular mechanism underlying this compensation is however still discussed controversially.[5-10] Thus, detailed molecular-level insight into how TMAO and urea interact in an aqueous environment is a key to understanding their role as chemical chaperones to maintain protein functionality. In the context of synthetic biology, such understanding is a prerequisite for the design of synthetic chaperones.

TMAO-urea interactions in an aqueous environment have been studied by focusing on the TMAO-water interaction,[11-14] urea-water interaction,[13, 15-19] and TMAO-urea interaction,[9, 19-22] using various techniques including pump-probe spectroscopy, neutron scattering, and molecular dynamics (MD) simulations. Also, the effects of TMAO and urea on protein structures in aqueous solution have been examined.[2, 4, 23-29] Regarding TMAO-urea interactions, previous studies using force field MD (FFMD) simulations[7, 9] and neutron scattering measurements[7] have proposed that TMAO and urea interact through the hydrogen-bond (H-bond) between the N_{UREA}-H_{UREA} groups of urea and the hydrophilic O_{TMAO}-N_{TMAO} group. Here,

N_{UREA} (H_{UREA}) denotes the nitrogen (hydrogen) atom of urea and O_{TMAO} (N_{TMAO}) denotes the oxygen (nitrogen) atom of TMAO. Other studies have concluded that TMAO and urea form no direct H-bonds but their effect on water and biomolecules is independent of each other.[6, 21] From a computational perspective, TMAO and urea force field models substantially influence the simulation results.[30] As such, the precise modeling of TMAO-urea interaction and the associated molecular conformation have remained elusive.

Here, by combining free energy calculations using *ab initio* MD (AIMD) simulations together with time-resolved infrared (TR-IR) spectroscopy and nuclear magnetic resonance (NMR) spectroscopy, we elucidate the preferred conformation of the TMAO-urea complex in water and the underlying mechanism for the TMAO-urea interaction. AIMD allows us to sample molecular conformations based on electronic structure theory, providing a more robust description of TMAO solvation dynamics than that obtained with FFMD.[31-33] Our AIMD simulations indicate that TMAO and urea prefer interacting via hydrophobic interaction, as opposed to recent reports.[6, 7, 9, 10, 22] Experimental TR-IR studies of water dynamics in aqueous TMAO-urea solutions confirm that TMAO preferentially H-bonds to water, rather than to urea. The NMR experiments provide evidence for the close proximity between urea and the hydrophobic methyl groups of TMAO. Our analysis uncovers that the large discrepancy between the H-bond strength of the strongly accepting O_{TMAO} atom and the weakly donating H_{UREA} atom prohibits the direct H-bonded TMAO-urea interaction.

RESULTS

To explore the free energy landscape of the TMAO-urea interaction and the molecular conformations in aqueous solution, we examine the interaction potential as a function of the separation between TMAO and urea in aqueous solution. Therefore, we calculated the potential of mean force (PMF) by varying the intermolecular distance (r) between the O_{TMAO} atom and the carbon atom of urea (C_{UREA}). Details are provided in Simulation Procedures and Supplemental Information. First, we compare the calculated free energy landscape of the AIMD and FFMD simulations. Figure 1 shows the simulated PMFs of the TMAO-urea interaction. Both AIMD and FFMD PMFs have a minimum at a distance of 5.3 Å $\leq r \leq$ 5.7 Å (the green shaded region), while the PMFs differ substantially at shorter TMAO-urea distances (r < 5.3 Å); the AIMD PMF suggests that the TMAO-urea interaction becomes increasingly unfavorable with decreasing r, while the FFMD simulation predicts the most stable TMAO-urea conformation is located at r = 4.1 Å (the yellow shaded region). Note that our study employed the AIMD simulation within the generalized gradient approximation for exchange-correlation functionals. A future challenge is thus to perform the PMF calculations with more sophisticated *ab initio* models (e.g., hybrid generalized gradient

approximations).[34] Nevertheless, the similarity of the PMFs obtained using different functionals (BLYP[35, 36] and revPBE[37] with Grimme's D3 correction[38]) suggests that the general shape is not critically affected by the choice of the functional.

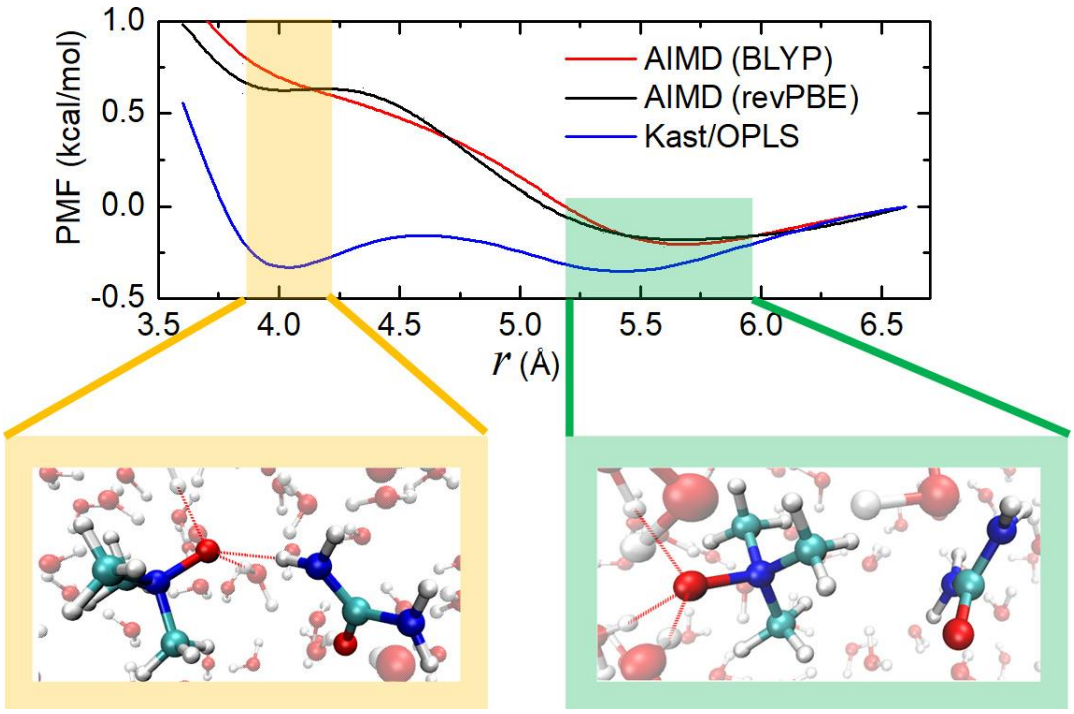

Figure 1. PMFs computed from AIMD and Kast/OPLS FFMD simulations. The typical conformations corresponding to the two PMF minima in the FFMD simulation are highlighted. The direct, H-bonded interaction predicted by FFMD (yellow highlight) is absent for the AIMD results, which predicts hydrophobic interaction (green highlight). See also Figures S5 and S8 in the Supplemental Information.

A detailed analysis of the molecular conformation at the energetic minimum 5.3 Å ≤ r ≤ 5.7 Å reveals that the TMAO-urea interaction is hydrophobic: the methyl groups of TMAO are facing urea, and the interaction is favored by dispersion interactions (see Sections 1-d and 1-k as well as Figures S11 of Supplemental Information). Conversely, a direct $O_{TMAO}\cdots H_{UREA}$ H-bond is formed between TMAO and urea for the FFMD energetic minimum at r = 4.1 Å (see Sections 1-k and 1-l as well as Figure S12 of Supplemental Information). These conformations are schematically depicted in the lower panels of Figure 1. In the following, we investigate the formation mechanism of the different structures predicted by the FFMD and AIMD simulations, by varying the charge distributions of TMAO and urea in the FFMD simulations.

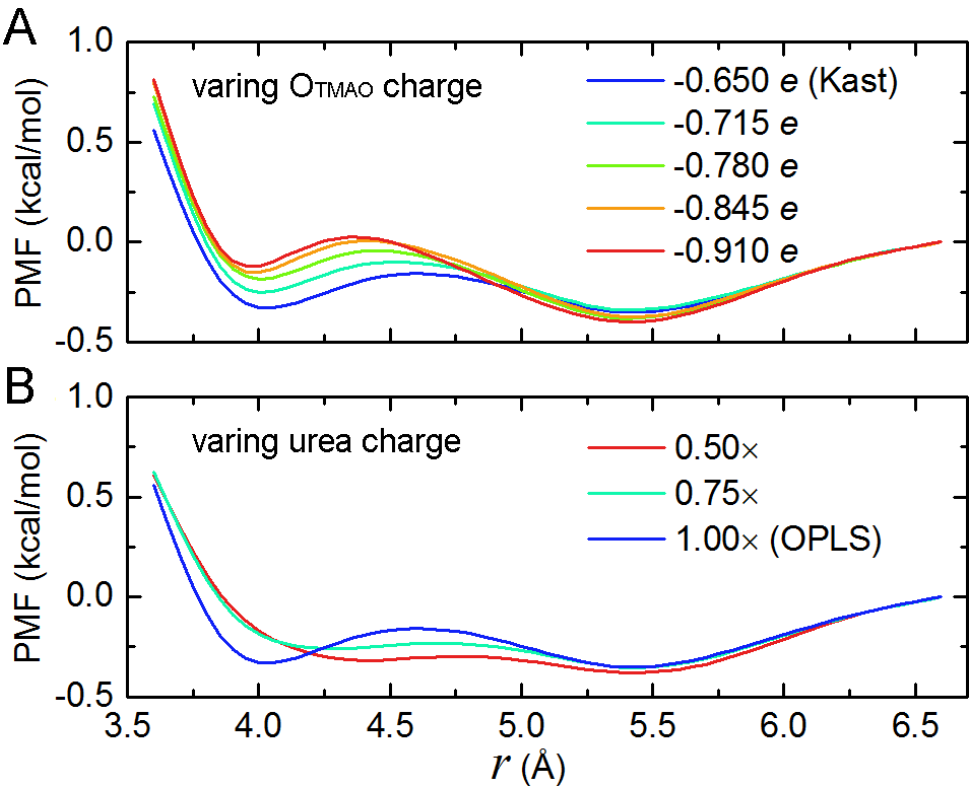

Figure 2. Variation of PMFs by controlling the hydrophilicity of the TMAO and urea. (A) Varying O_{TMAO} and N_{TMAO} atom charges of the Kast TMAO model. (B) Varying atom charges of the OPLS urea model.

As the partial charge of the O_{TMAO} atom critically affects the H-bond strength of TMAO,[39, 40] we explore how the variation of this charge affects the FFMD PMFs. We calculated the PMFs by systematically varying the charge of O_{TMAO} from -0.65 *e* (as implemented in the Kast model[41]) to -0.91 *e* (used in the Netz model[39]). Here, the charges of the C_{TMAO} and H_{TMAO} atoms were fixed, while the charge assigned to the N_{TMAO} atom was adjusted to ensure charge neutrality of TMAO. The increased partial charge on the O_{TMAO} atom enhances the H-bond accepting strength of TMAO.[32] Nevertheless, counter-intuitively, the enhanced H-bond accepting strength of TMAO destabilizes the TMAO-urea H-bond interaction in water. As can be seen from the simulated PMFs in Figure 2A, an increase in the partial charge on the O_{TMAO} atom elevates the PMF at r = 4.1 Å, while it does not substantially affect the PMF at r = 5.3 Å. Despite the increase of the H-bonding strength of TMAO, the H-bonded TMAO-urea complex is destabilized, while not affecting the hydrophobic complex.

Subsequently, we focus on the effects of the charge distribution of urea on the PMFs by scaling the atom charges of the OPLS urea model. We increased the partial charge of H_{UREA}, thereby increasing the H-bond donating strength of urea. The simulated PMFs (Figure 2B) show that a higher partial charge on the H_{UREA} atom lowers the PMF at r = 4.1 Å: a stronger H-bond donating urea intuitively stabilizes the directly H-bonded TMAO-urea conformation.

This opposite effect of increasing the H-bonding strengths of TMAO and urea on the stability of their H-bonded conformation obviously cannot be explained solely from their pair interaction potential; the increase in the absolute value of charges on either O_{TMAO} or H_{UREA} strengthens the $O_{TMAO}\cdots H_{UREA}$ H-bond. Consequently, the data suggest that water plays a key role in the (de-)stabilization of the $O_{TMAO}\cdots H_{UREA}$ H-bond, specifically the $O_{TMAO}\cdots H_W$ and $H_{UREA}\cdots O_W$ H-bond interactions, where H_W and O_W denote the H and O atoms of the water molecule, respectively. To assess the relative strengths of the TMAO-water, water-water, and urea-water H-bonds, we compute the H-bond time correlation function;[42]

$$P_{\mathrm{HB}}(t) = \frac{\langle h(0)h(t)\rangle}{\langle h(0)\rangle} \qquad \text{(Equation 1)}$$

$h(t)$ is unity when 1.59 Å < $r_{O\cdots H}$ < 2.27 Å, 0 otherwise, where $r_{O\cdots H}$ denotes the intermolecular distance between O and H atoms. Slower decay of $P_{\mathrm{HB}}(t)$ indicates a longer-lived, stronger H-bond.

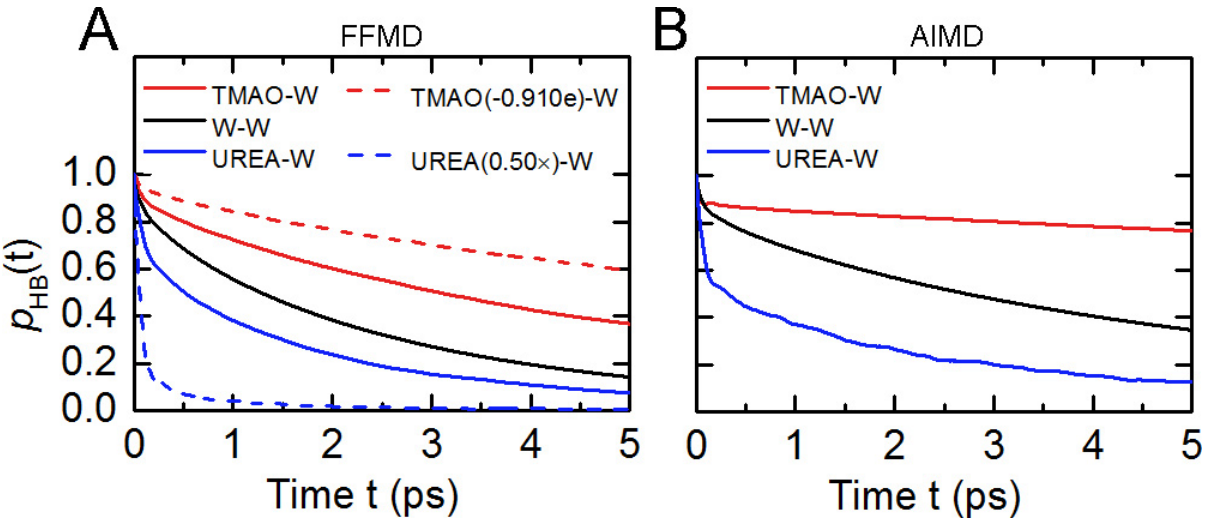

Figure 3. H-bond time correlation functions reveal the hydrophilicity/hydrophobicity of TMAO and urea. (A) FFMD data of aqueous TMAO solutions (TMAO-W), aqueous urea solutions (UREA-W), and pure water (W-W), where W stands for water. The data with scaled charge are also plotted. See also Figure S6 in the Supplemental Information. (B) corresponding AIMD (BLYP) data.

Figure 3A shows the FFMD data of the $O_{TMAO}\cdots H_W$, $O_W\cdots H_W$, and $H_{UREA}\cdots O_W$ H-bond time correlation functions. The H-bond lifetime increases in the order of $\tau_{UREA\text{-}W} < \tau_{W\text{-}W} < \tau_{TMAO\text{-}W}$, indicating that the H-bond strength increases in the order of $H_{UREA}\cdots O_W$, $O_W\cdots H_W$, and $O_{TMAO}\cdots H_W$. When the absolute value of the O_{TMAO} partial charge is increased, the $O_{TMAO}\cdots H_W$ H-bond dynamics slows down even more. Similarly, the decrease in H_{UREA} partial charge accelerates the $H_{UREA}\cdots O_W$ H-bond dynamics. As such, an increase in the absolute value of the O_{TMAO} charge (decrease in the H_{UREA} charge) enhances the difference between $O_{TMAO}\cdots H_W$ ($H_{UREA}\cdots O_W$) and $O_W\cdots H_W$ H-bond strength and lifetimes. Apparently, as the PMFs

in Figure 2 reveal, the enhanced differences in the H-bond strengths of $O_{TMAO}\cdots H_W$ and $O_W\cdots H_W$ and those of $H_{UREA}\cdots O_W$ and $O_W\cdots H_W$ both destabilize the directly H-bonded TMAO-urea conformation.

Why does such enhanced difference of TMAO-water or urea-water H-bonds relative to water-water H-bonds destabilize the TMAO-urea conformation? This can be understood as follows: an increase in the absolute value of the O_{TMAO} charge makes the $O_{TMAO}\cdots H_W$ interaction more favorable than the $O_{TMAO}\cdots H_{UREA}$ interaction, as the difference in the interaction energy increases due to the enhanced electrostatic contributions. The decrease in the H_{UREA} charge also makes the $O_{TMAO}\cdots H_W$ interaction more favorable than the $O_{TMAO}\cdots H_{UREA}$ interaction, since the $O_{TMAO}\cdots H_{UREA}$ interaction is destabilized.

Based on this understanding, we turn our focus to the AIMD H-bond dynamics in Figure 3B. The differences between the $O_{TMAO}\cdots H_W$, $O_W\cdots H_W$, and $H_{UREA}\cdots O_W$ H-bond dynamics are more pronounced in the AIMD simulation than in the FFMD simulation. These variations in inferred H-bond strengths are corroborated by the conformational energy data obtained by force field and density functional theory (DFT) calculations (see Sections 1-k and 1-l of Supplemental Information). Based on the above notion, the enhanced difference in the H-bond strengths of TMAO and urea in the AIMD simulation leads to an even more unfavorable H-bonded interaction of TMAO-urea, consistent with the PMF (Figure 1). As such, our AIMD results show that the O_{TMAO} atom is preferentially H-bonded to water molecules in aqueous solutions of TMAO and urea, in contrast to previous reports based on FFMD results.[7, 9, 30] Because of the unstable H-bonded TMAO-urea conformation, the hydrophobic association of TMAO and urea becomes the only favorable TMAO-urea conformation.

Experiments support the conclusion that TMAO and urea interact hydrophobically, rather than through H-bonding interaction in the aqueous mixture. As discussed below, polarization-resolved femtosecond infrared pump-probe experiments[43, 44] reveal that TMAO H-bonds preferentially with water, rather than with urea. The results of NMR experiments are likewise consistent with the hydrophobic interactions between TMAO and urea.

In the femtosecond TR-IR experiments, the effect of TMAO and urea on the dynamics of water is investigated. In these experiments, an intense IR pulse excites the O-D stretch vibration for HOD molecules diluted in H_2O. Since O-D oscillators parallel to the laser pulse polarization are preferentially excited, the excitation is anisotropic. Due to the random orientational motion of water, the anisotropy decays (with a decay time of ~2 ps for pure water). Experimental details are provided in Supplemental Information.

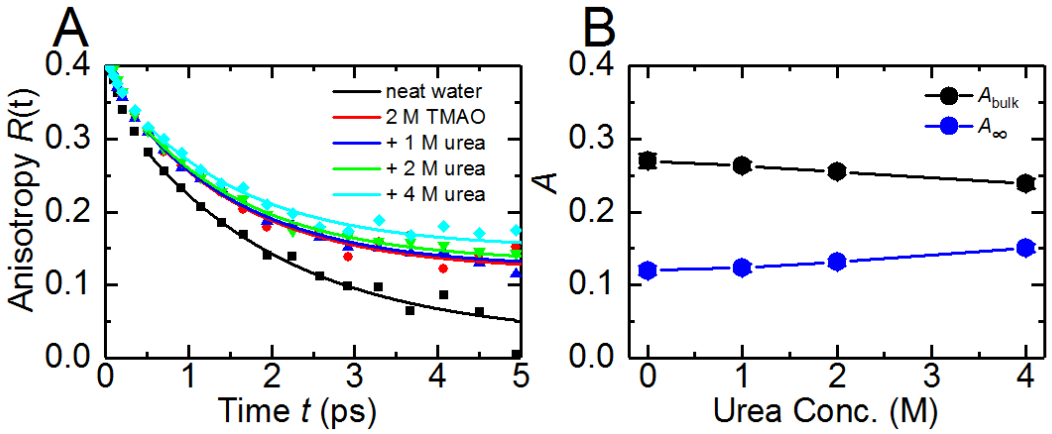

Figure 4. TR-IR experiments indicates the unfavorable H-bonded TMAO-urea conformation. (A) Decay of the excitation anisotropy $R(t)$ of the O-D stretching vibration (2470 – 2530 cm^{-1}) for neat water (black), 2 M TMAO (red), 2 M TMAO/1 M urea (blue), 2 M TMAO/2 M urea (green) and 2 M TMAO/4 M urea (cyan). The solid lines show fits of a mono-exponential decays with an offset ($R(t) = A_{bulk} \exp(-t/\tau_{rot})+A_\infty$) to the data.[43] (B) Values of A_∞ and A_{bulk} for aqueous TMAO solutions (2 M) with different concentrations of urea. See also Figure S13 in the Supplemental Information.

The anisotropy decay data are displayed in Figure 4A. The comparison of neat water (black) and aqueous TMAO solution (red) indicates that the presence of TMAO causes the orientational motion of a significant fraction of the O-D groups to be slowed down substantially, with no reorientation discernible within the experimentally accessible time window of ~5 ps.[43] This "immobilization" is caused by the formation of strong, long-lived $O_{TMAO}\cdots H_W$ H-bonds.[11, 44] To quantify the fraction of immobilized water, we fit a mono-exponential decay with an offset (A_∞) to the experimental data, where A_∞ is proportional to the number of immobilized water molecules.[17] These fits confirm the qualitative observations: 2 M TMAO immobilizes 30% of the water molecules (A_∞ = 0.12 out of 0.4) (see Figure 4B). As the observed immobilization of water dynamics due to TMAO predominately originates from the strong H-bonds between O_{TMAO} and water, the insensitivity of water rotational motion towards urea indicates that the long-lived $O_{TMAO}\cdots H_W$ H-bonds stay intact for all studied solutions. Thus, in line with the AIMD results, the rotational dynamics of water as measured with IR pump-probe spectroscopy provides experimental evidence for the absence of direct H-bonds formed between TMAO and urea, which would release HOD molecules bonded to TMAO and thus speed up water dynamics. This notion is consistent with an earlier dielectric relaxation study.[22] Contrarily, the observed slowing-down upon addition of urea to a 2M solution of TMAO is in quantitative agreement (an increase of A_∞ by ~0.03 upon addition of 4M urea) with what has been observed for aqueous solutions of only urea.[17] As such, the effect of TMAO and urea on water dynamics is found to be simply additive. This observation indicates that the TMAO-urea interaction does not involve

water and that the TMAO-urea interaction does not affect the interaction of the two molecules individually with water. Hence, this is fully consistent with the TMAO-urea interaction occurring through hydrophobic moieties.

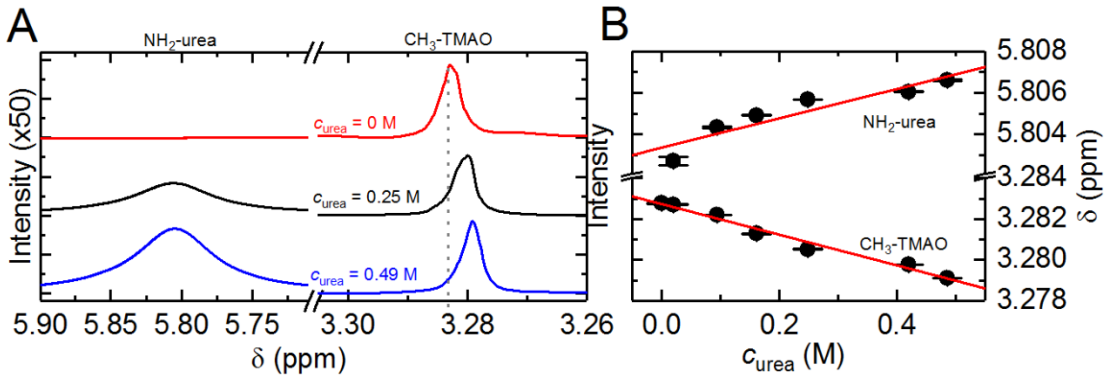

Figure 5. NMR chemical shift further supports the hydrophobic association between TMAO and urea. (A) ^{1}H-NMR spectra for solutions of TMAO (c_{TMAO} = 0.35 M) with increasing concentration of urea. The peaks at ~3.28 ppm correspond to the CH_3 protons of TMAO, which shift up-field upon addition of urea. The peaks at ~5.8 ppm can be assigned to urea. (B) Extracted chemical shift of the CH_3 protons and chemical shift of the NH_2 groups of urea as a function of c_{urea} at a constant concentration of TMAO (c_{TMAO} = 0.35 M). The red lines are guides to the eye. Error bars correspond to the square root of the diagonal element of the covariance matrix when fitting a Lorentzian line to the peak and thus represent a measure for the experimental precision. See also Figure S14 in the Supplemental Information.

Experimental and computational NMR data further support the conclusion that TMAO and urea interact via the hydrophobic CH_3 groups of TMAO. ^{1}H NMR spectra of solutions with 0.35 M TMAO indicate that the chemical shift of the CH_3 group of TMAO shifts up-field with increasing concentration of urea (from 0 to 0.49 M urea, see Figure 5, for experimental details see Supplemental Information). In contrast, the protons of urea undergo a minor down-field shift (Figure 5). *Ab initio* calculations for the chemical shift of TMAO ^{1}H chemical shift (see Supplemental Information) indicate that this up-field shift of TMAO's protons arises from the proximity of urea to TMAO's CH_3 groups. For substitution of a water-TMAO (H_W…O_{TMAO}) H-bond by a urea-TMAO (H_{UREA}…O_{TMAO}) H-bond, a down-field shift of the TMAO's CH_3 groups would be expected. Although it is generally extremely challenging to directly prove intermolecular interactions using NMR for such weak association,[45] the NMR spectra together with the chemical shift calculations provide evidence for the proximity of urea to TMAO's CH_3 groups. Thus, the NMR chemical shifts are also consistent with the hydrophobic interaction between TMAO and urea.

DISCUSSION

As is shown above, the orthogonal prediction of favorable TMAO-urea H-bonded conformation by FFMD[7, 9] arises from the inaccurate Kast model of TMAO and OPLS model of urea. In fact, it is known that these models cannot reproduce the vibrational signature of water in the aqueous TMAO solution.[11, 46] Furthermore, urea is too hydrophilic when the OPLS model is used.[15] Such a combination of force field models misrepresented the physical picture of TMAO-urea conformation. Furthermore, the radial distribution function of water-water in the aqueous TMAO solution measured by neutron scattering measurement is ill-defined when varying the concentration of solute. Indeed, by increasing the urea concentration, one can expect that the hydration number of water-water reduces, which is consistent with the neutron-scattering data. Thus, the reduction of the hydration number of water-water does not necessarily indicate that urea progressively replaces the water molecules in the first coordination shell of the TMAO oxygen atom.[6] Our NMR/TR-IR measurements can probe such TMAO-urea conformation more clearly.

The observation of the hydrophobic interaction between TMAO and urea has three major implications. (1) The (ensemble) averaged strength of all H-bonds that water forms is correlated to the solution osmotic coefficient. In urea solution, the H-bond strength of water is reduced, as urea-water H-bonds are weaker than water-water H-bonds and thus decrease the osmotic coefficient. TMAO can counter this decrease in the osmotic stress due to urea, by forming stronger H-bonds to water than water-water H-bonds. Our findings thus provide a rationale for the counteracting effects of TMAO and urea on the osmotic stress. This counteraction occurs via independent interaction of urea and TMAO with water, which is in line with the conclusions from experimental measurements of the osmotic pressure for TMAO-urea solutions.[10] (2) We observed that, the hydrophobic TMAO-urea interactions are more favorable than their H-bonding interaction. This hydrophobic interaction between TMAO and urea can thus explain the non-ideal behavior of the viscosity and the molecular rotation times of TMAO and urea in aqueous solution, which some of us have ascribed previously to water mediated interactions between TMAO and urea.[22] Along those lines, Rösgen and Jackson-Atogi have shown that TMAO behaves like hard-sphere with two hydration sites which can be replaced by urea.[10] Our results show that the hydration sites where urea replaces water are located at the hydrophobic methyl groups of TMAO instead of the previously supposed hydrophilic part. (3) The hydrophobic TMAO-urea interaction might be counterintuitive at first sight, since urea does not have any specific hydrophobic (e.g., methyl) groups. The weak H-bond acceptor and donor strength together with urea's rather planar geometry, makes it difficult to incorporate urea into the H-bonded structure of water. This leads to rather hydrophobic behavior of urea where dispersion interactions are important, which has recently been confirmed from experiments using thermodiffusion.[47]

In summary, our combined AIMD, ultrafast polarization-resolved infrared measurement, and NMR measurement show that TMAO does not directly H-bond with urea in aqueous solution, in contrast to conclusions from previous FFMD studies. The unfavorable direct TMAO-urea interactions can be traced back to the large difference in their H-bonding abilities: TMAO-water H-bonds are much stronger than urea-water H-bonds. The TMAO-urea interaction is more favored by hydrophobic interaction between the methyl groups of TMAO and urea, and thus water molecules H-bonded to TMAO are *not* replaced by urea. Our results show that the different, compensatory osmotic effect of TMAO and urea stems from their individual and independent interactions with water.

SIMULATION PROCEDURES

PMF calculation

We computed the PMF via the thermodynamic integration:[48]

$$W(r) = -\int_{r_0}^{r} \langle F(r') \rangle dr' + 2k_B T \ln\left(\frac{r}{r_0}\right) \qquad \text{(Equation 2)}$$

where $2k_B T \ln(r/r_0)$ represents the contribution of the volume-entropy, $F(r)$ is the force acting between the constrained C_{UREA} and O_{TMAO} atoms when the O_{TMAO}-C_{UREA} distance is equal to r, and r_0 represents the maximum O_{TMAO}-C_{UREA} separation for calculating the PMF. We constrained the distance between O_{TMAO} and C_{UREA} ranging from 3.60 to 6.60 Å with an interval of 0.25 Å. The constraint was made by using the SHAKE algorithm.[49] The choice of reaction coordinate, the effect of the elevated temperature on the PMF, and the effect of simulation cell size on the PMF are illustrated in Figure S1, S2, and S3, respectively.

FFMD simulation

We used the Kast model for TMAO,[41] the OPLS model for urea,[50] and SPC/E model for water[51] in force field molecular dynamics (FFMD) simulation. Such a combination of force field models has been used to show the strong direct hydrogen-bond (H-bond) between TMAO and urea.[9] Furthermore, we used two different TMAO models (the Shea model[40] and the Netz model[39]) and one urea model (the Kirkwood-Buff (KB) model[15]). The combination rules used for the LJ interactions in this study are as follows: $\sigma_{ij} = \sqrt{\sigma_i \sigma_j}$ and $\epsilon_{ij} = \sqrt{\epsilon_i \epsilon_j}$, where σ_i denotes the van der Waals (vdW) radius of atom i, and ϵ_i denotes the well depths of atom i. Such combination rules were also adopted in a recent study of association of hydrophobic molecules in TMAO-urea-water solution.[30]

For the analyses in Figure 2A, we varied the charges of the O_{TMAO} and N_{TMAO} atoms in the Kast model.[41] The charges were obtained by combining the partial charges of the Kast model (q_{Kast})[41] and the Netz model (q_{Netz}).[39] In the Kast and the Netz TMAO models, the partial charges of the O_{TMAO} and N_{TMAO} atoms are different, while the partial charges of the C_{TMAO} and H_{TMAO} atoms are the same. By varying the partial charges, the hydrophilic part of the TMAO force field gradually changes from the Kast model to the Netz model.[39] Note that the Netz model is known to reproduce the H-bond dynamics of water.[32] We summarized the partial charges for TMAO models in Table S6 in the Supplemental Information. For the analyses in Figure 2B in the main text, we varied charges of urea by scaling the partial charges of the OPLS urea model[50] with different factors. We summarized the partial charges in the urea models in Table S7 in the Supplemental Information.

For all these simulations, temperature was controlled by using the thermostats of canonical sampling through velocity rescaling[52] with a time constant of 300 fs. The timestep for integrating the equation of motion was set to 0.5 fs. The CP2K software package[53] was used in all the FFMD simulations. Further details on the simulation protocols are presented in Sections 5-a, b, c, d, e in Supplemental Information.

We further analyzed the effects of the LJ radii of the C_{TMAO} and H_{TMAO} atoms in the Kast model on the PMF (see Table S1 and Figure S2 in Supplemental Information) and the PMFs computed with other combinations of the force field models of TMAO and urea (Figure S3 in the Supplemental Information). The H-bond dynamics of the OPLS urea and the KB urea models (see Figure S5 in the Supplemental Information) and the conformation energies of H-bonded dimer of TMAO-urea and TMAO-water (see Table S2 in the Supplemental Information) are consistent with our rational of the difference of force fields.

AIMD simulation

In AIMD simulations, all the molecules were deuterated. The Born-Oppenheimer AIMD simulations were performed with density functional theory. For the exchange and correlation functional, we used the Becke[35]/Lee-Yang-Parr [36](BLYP) and revised Perdew–Burke–Ernzerhof (revPBE)[37] functionals together with the van der Waals correction of the Grimme's D3 method.[38] The van der Waals corrections are crucial to reproduce the correct water density and dynamics.[54-56] We employed the Goedecker-Teter-Hutter pseudopotentials[57] and the hybrid Gaussian and plane waves method. The TZV2P basis sets were used for the Gaussian wave functions. A 320 Ry cutoff was used for the auxiliary plane waves. Periodic boundary conditions were employed. The temperature was controlled by using the thermostats of canonical sampling through velocity rescaling[52] with a time constant of 300 fs. The timestep for integrating the

equation of motion was set to 0.5 fs. The QUICKSTEP module implemented in the CP2K software package[53] was used in all the AIMD simulations. The convergence of the limited AIMD trajectory was examined in Sections 1-h and 1-i as well as Figures S8-S10 in Supplemental Information. Further details on the simulation protocols are presented in Sections 5-b, c, d, e in Supplemental Information.

We note that since the computational cost for AIMD simulation for TMAO-urea aqueous solutions is huge, we used the exchange-correlation functionals within the generalized gradient approximation (GGA) such as BLYP and revPBE. Recently, the high-level computation with hybrid GGA was used for computing the simple NaCl aqueous solution,[34] which is however ~10 times more demanding, compared to the GGA-AIMD simulation. Thus, in this study, we compared the accuracy of the GGA functionals by comparing the conformational energy of TMAO and urea (see Tables S3 and S4 in the Supplemental Information). Calculating the PMF with hybrid GGA would be thus a future challenge.

EXPERIMENTAL PROCEDURES

Polarization-resolved femtosecond infrared pump-probe experiments

Femtosecond laser pulses from a regenerative amplifier (Spectra Physics, Spitfire Ace, 800 nm, 35 fs, 1 kHz repetition rate) were converted into mid-IR pulses (ω = 2500 cm^{-1} peak frequency and ~ 400 cm^{-1} FWHM) using an optical parametric amplifier together with a difference frequency generation stage (Light conversion, TOPAS) and split into pump and probe pulses. A half-wave plate was used to rotate the pump polarization to 45° with respect to the probe polarization. The timing of the pump pulses was delayed relative to the probe pulse using a translational stage and both the pump and the probe pulses are focused into the sample and re-collimated using off-axis parabolic mirrors. For the probe pulse, the component parallel and perpendicular to the pump polarization can be selected by using a polarizer, giving the parallel ($\Delta a_{\parallel}(\omega, t)$) and perpendicular ($\Delta a_{\perp}(\omega, t)$) transient (pump-induced) absorption spectra, respectively. Both components were spectrally dispersed onto a 2 × 32 MCT (mercury-cadmium-telluride) array, where both the intensity with and without the pump is detected (I_{probe}). For active noise reduction a reference beam was detected simultaneously and the pump beam was modulated at 500Hz using an optical chopper.

The transient absorption of the samples is given by

$$\Delta a = -\ln[I_{\mathrm{probe,with\ pump}}/I_{\mathrm{probe,without\ pump}}]. \qquad \text{(Equation 3)}$$

Isotropic transient absorption, which does not contain rotational contributions, but represents only energy relaxation and dissipation

$$\Delta a_{iso}(\omega,t) = \frac{\Delta a_{\parallel}(\omega,t)+2\Delta a_{\perp}(\omega,t)}{3} \quad \text{(Equation 4)}$$

was constructed and fitted by a two-step relaxation model to extract the contributions of vibrational excitation and the heating to the signal.[58] The dynamics of isotropic component is shown in Figure S13 in the Supplemental Information.

The anisotropy of the excitation, as shown in the main manuscript, $R(\omega,t)$ was calculated by

$$R(\omega,t) = \frac{\Delta a_{\parallel}'(\omega,t)-\Delta a_{\perp}'(\omega,t)}{\Delta a_{\parallel}'(\omega,t)+2\Delta a_{\perp}'(\omega,t)}, \quad \text{(Equation 5)}$$

where $\Delta a_{\parallel}'(\omega,t)$ and $\Delta a_{\perp}'(\omega,t)$ correspond to the parallel and perpendicular transient spectra, corrected for the heating contributions (for details see Refs. 17, 43).

We used Trimethylamine-N-oxide dihydrate (SigmaAldrich, >99%) and urea (SigmaAlrich >99%) without further purification. All samples were prepared by weighing the appropriate amount of trimethylamine-N-oxide dihydrate and urea into volumetric flask and mixing them with 5wt% heavy water (SigmaAldrich, 99.9 %D) in Milli-Q water (Millipore, 18.2 MΩ cm at 25 deg).

^{1}H NMR measurement

To determine the chemical environment of the hydrophobic CH_3 groups of TMAO as a function of urea concentration we performed ^{1}H-NMR experiments. ^{1}H-NMR spectra of the solutions in H_2O were recorded using a 850 MHz Bruker AVANCE III system equipped with a 5 mm triple resonance TXI ^{1}H/^{13}C/^{15}N probe with a *z*-gradient. For the proton NMR spectra 16 to 64 transients (depending on the urea concentration) using a 9 μs long 90° pulse and a 17000 Hz spectral width together with a recycling delay of 10 s. For referencing, a sealed capillary with DMSO-d_6 was placed inside the 5 mm tube with a small fraction of DMSO-d_5H. Since the local magnetic field inside and outside the capillary may differ, we measured a neat water sample with the DMSO-d_6 capillary inside to account for the difference in magnetic field. We calibrate the DMSO-d_5H signal to 3.05 ppm, such that the peak of H_2O in neat water is centred at 4.8 ppm. All subsequent samples were referenced based on the DMSO-d_5H signal at 3.05 ppm. Using this referencing approach, the observed chemical shift of TMAO's CH_3 groups at ~3.28ppm is in broad agreement with previous studies.[59] The temperature was controlled to 298.3 K with a VTU (variable temperature unit) and an accuracy of +/- 0.1 K. Experiments were performed using a constant

concentration of TMAO (0.35 M) with increasing concentration of C13-urea (0-0.49 M). The data of other hydrogen atoms (DMSO and urea) are shown in Figure S14 in the Supplemental Information.

The *ab initio* calculation of the chemical shift is described in Section 4, Figure S15, Table S5 in Supplemental Information.

SUPPLEMENTAL INFORMATION

Supplemental Information includes simulation details, supplemental data of simulations, TR-IR experimental data, NMR experimental data, and computational of the NMR chemical shift, together with 7 tables and 15 figures can be found online with this article online at https://doi.org/10.1016/j.chempr.2018.08.020

ACKNOWLEDGMENT

We thank Prof. Hans Wolfgang Spiess for fruitful discussion. We are thankful to the computational resources of Max Planck Computing and Data Facility. SC and JH acknowledge financial support from the European Research Council (ERC) under the European Union's Horizon 2020 research and innovation program (grant agreement no 714691). TO thanks computational resources at the Cybermedia Center, Osaka University, Japan. YM acknowledges the computational resources of the HPC Cluster in the Lawrence Berkeley National Laboratory of USA. WJX acknowledges financial support by the graduate school of Peking University and the Max Planck Institute for Polymer Research.

AUTHOR CONTRIBUTIONS

WJX, JH, YN, and MB conceived the research idea, WJX, TO, WM, YM and YN performed the simulation and additional calculations, SC and MW performed the experiment, WJX, SC, JH, YN analyzed the data, and all the authors wrote the manuscript.

DECLARATION OF INTERESTS

The authors declare no competing interests.

REFERENCES AND NOTES

1. Yancey, P. H. (2001). Water stress, osmolytes and proteins. Am Zool 41, 699-709.
2. Canchi, D. R., and Garcia, A. E. (2013). Cosolvent effects on protein stability. Annu Rev Phys Chem 64, 273-293.
3. Levine, Z. A., Larini, L., LaPointe, N. E., Feinstein, S. C., and Shea, J. E. (2015). Regulation and aggregation of intrinsically disordered peptides. Proc Natl Acad Sci USA 112, 2758-2763.
4. Ganguly, P., Hajari, T., Shea, J. E., and van der Vegt, N. F. A. (2015). Mutual exclusion of urea and trimethylamine N-oxide from amino acids in mixed solvent environment. J Phys Chem Lett 6, 581-585.
5. Zou, Q., Bennion, B. J., Daggett, V., and Murphy, K. P. (2002). The molecular mechanism of stabilization of proteins by TMAO and its ability to counteract the effects of urea. J Am Chem Soc 124, 1192-1202.
6. Meersman, F., Bowron, D., Soper, A. K., and Koch, M. H. J. (2011). An X-ray and neutron scattering study of the equilibrium between trimethylamine N-oxide and urea in aqueous solution. Phys Chem Chem Phys 13, 13765-13771.
7. Meersman, F., Bowron, D., Soper, A. K., and Koch, M. H. J. (2009). Counteraction of urea by trimethylamine N-oxide is due to direct interaction. Biophys J 97, 2559-2566.
8. Graziano, G. (2011). How does trimethylamine N-oxide counteract the denaturing activity of urea? Phys Chem Chem Phys 13, 17689-17695.
9. Paul, S., and Patey, G. N. (2007). Structure and interaction in aqueous urea-trimethylamine-N-oxide solutions. J Am Chem Soc 129, 4476-4482.
10. Rosgen, J., and Jackson-Atogi, R. (2012). Volume exclusion and H-bonding dominate the thermodynamics and solvation of trimethylamine-N-oxide in aqueous urea. J Am Chem Soc 134, 3590-3597.
11. Usui, K., Hunger, J., Sulpizi, M., Ohto, T., Bonn, M., and Nagata, Y. (2015). Ab initio liquid water dynamics in aqueous TMAO solution. J Phys Chem B 119, 10597-10606.
12. Ohto, T., Hunger, J., Backus, E. H., Mizukami, W., Bonn, M., and Nagata, Y. (2017). Trimethylamine-N-oxide: Its hydration structure, surface activity, and biological function, viewed by vibrational spectroscopy and molecular dynamics simulations. Phys Chem Chem Phys 19, 6909-6920.
13. Pazos, I. M., and Gai, F. (2012). Solute's perspective on how trimethylamine oxide, urea, and guanidine hydrochloride affect water's hydrogen bonding ability. J Phys Chem B 116, 12473-12478.
14. Kundu, A., Verma, P. K., and Cho, M. (2018). Effect of osmolytes on the conformational behavior of a macromolecule in a cytoplasm-like crowded environment: A femtosecond mid-IR pump-probe spectroscopy study. J Phys Chem Lett 9, 724-731.
15. Weerasinghe, S., and Smith, P. E. (2003). A Kirkwood-Buff derived force field for mixtures of urea and water. J Phys Chem B 107, 3891-3898.
16. Carr, J. K., Buchanan, L. E., Schmidt, J. R., Zanni, M. T., and Skinner, J. L. (2013). Structure and dynamics of urea/water mixtures investigated by vibrational spectroscopy and molecular dynamics simulation. J Phys Chem B 117, 13291-13300.
17. Rezus, Y. L. A., and Bakker, H. J. (2006). Effect of urea on the structural dynamics of water. Proc Natl Acad Sci USA 103, 18417-18420.
18. Lee, H., Choi, J. H., Verma, P. K., and Cho, M. (2015). Spectral graph analyses of water hydrogen-bonding network and osmolyte aggregate structures in osmolyte-water solutions. J Phys Chem B 119, 14402-14412.
19. Samanta, N., Das Mahanta, D., and Kumar Mitra, R. (2014). Does urea alter the collective hydrogen-bond dynamics in water? A dielectric relaxation study in the terahertz-frequency region. Chem Asian J 9, 3457-3463.
20. Rezus, Y. L., and Bakker, H. J. (2009). Destabilization of the hydrogen-bond structure of water by the osmolyte trimethylamine n-oxide. J Phys Chem B 113, 4038-4044.
21. Sahle, C. J., Schroer, M. A., Juurinen, I., and Niskanen, J. (2016). Influence of TMAO and urea on the structure of water studied by inelastic X-ray scattering. Phys Chem Chem Phys 18, 16518-16526.
22. Hunger, J., Ottosson, N., Mazur, K., Bonn, M., and Bakker, H. J. (2015). Water-mediated interactions between trimethylamine-N-oxide and urea. Phys Chem Chem Phys 17, 298-306.
23. Kokubo, H., Hu, C. Y., and Pettitt, B. M. (2011). Peptide conformational preferences in osmolyte solutions: Transfer free energies of decaalanine. J Am Chem Soc 133, 1849-1858.

24. Bennion, B. J., and Daggett, V. (2004). Counteraction of urea-induced protein denaturation by trimethylamine N-oxide: A chemical chaperone at atomic resolution. Proc Natl Acad Sci USA 101, 6433-6438.
25. Ma, J., Pazos, I. M., and Gai, F. (2014). Microscopic insights into the protein-stabilizing effect of trimethylamine N-oxide (TMAO). Proc Natl Acad Sci U S A 111, 8476-8481.
26. Liao, Y. T., Manson, A. C., DeLyser, M. R., Noid, W. G., and Cremer, P. S. (2017). Trimethylamine N-oxide stabilizes proteins via a distinct mechanism compared with betaine and glycine. Proc Natl Acad Sci USA 114, 2479-2484.
27. Su, Z., Mahmoudinobar, F., and Dias, C. L. (2017). Effects of trimethylamine-N-oxide on the conformation of peptides and its implications for proteins. Phys Rev Lett 119, 108102.
28. Smolin, N., Voloshin, V. P., Anikeenko, A. V., Geiger, A., Winter, R., and Medvedev, N. N. (2017). TMAO and urea in the hydration shell of the protein snase. Phys Chem Chem Phys 19, 6345-6357.
29. Wei, H. Y., Fan, Y. B., and Gao, Y. Q. (2010). Effects of urea, tetramethyl urea, and trimethylamine N-oxide on aqueous solution structure and solvation of protein backbones: A molecular dynamics simulation study. J Phys Chem B 114, 557-568.
30. Ganguly, P., van der Vegt, N. F., and Shea, J. E. (2016). Hydrophobic association in mixed urea-TMAO solutions. J Phys Chem Lett 7, 3052-3059.
31. Imoto, S., Forbert, H., and Marx, D. (2015). Water structure and solvation of osmolytes at high hydrostatic pressure: Pure water and TMAO solutions at 10 kbar versus 1 bar. Phys Chem Chem Phys 17, 24224-24237.
32. Usui, K., Nagata, Y., Hunger, J., Bonn, M., and Sulpizi, M. (2016). A new force field including charge directionality for TMAO in aqueous solution. J Chem Phys 145, 064103.
33. Imoto, S., Kibies, P., Rosin, C., Winter, R., Kast, S. M., and Marx, D. (2016). Toward extreme biophysics: Deciphering the infrared response of biomolecular solutions at high pressures. Angew Chem Int Ed 55, 9534-9538.
34. Yao, Y., and Kanai, Y. (2018). Free energy profile of NaCl in water: First-principles molecular dynamics with SCAN and ωB97X-V exchange-correlation functionals. J Chem Theory Comput 14, 884-893.
35. Becke, A. D. (1988). Density-functional exchange-energy approximation with correct asymptotic-behavior. Phys Rev A 38, 3098-3100.
36. Lee, C. T., Yang, W. T., and Parr, R. G. (1988). Development of the Colle-Salvetti correlation-energy formula into a functional of the electron-density. Phys Rev B 37, 785-789.
37. Zhang, Y. K., and Yang, W. T. (1998). Comment on "generalized gradient approximation made simple". Phys Rev Lett 80, 890-890.
38. Grimme, S., Antony, J., Ehrlich, S., and Krieg, H. (2010). A consistent and accurate ab initio parametrization of density functional dispersion correction (DFT-D) for the 94 elements H-Pu. J Chem Phys 132, 154104.
39. Schneck, E., Horinek, D., and Netz, R. R. (2013). Insight into the molecular mechanisms of protein stabilizing osmolytes from global force-field variations. J Phys Chem B 117, 8310-8321.
40. Larini, L., and Shea, J. E. (2013). Double resolution model for studying TMAO/water effective interactions. J Phys Chem B 117, 13268-13277.
41. Kast, K. M., Brickmann, J., Kast, S. M., and Berry, R. S. (2003). Binary phases of aliphatic N-oxides and water: Force field development and molecular dynamics simulation. J Phys Chem A 107, 5342-5351.
42. Luzar, A., and Chandler, D. (1996). Hydrogen-bond kinetics in liquid water. Nature 379, 55-57.
43. Rezus, Y. L. A., and Bakker, H. J. (2007). Observation of immobilized water molecules around hydrophobic groups. Phys Rev Lett 99, 148301.
44. Hunger, J., Tielrooij, K. J., Buchner, R., Bonn, M., and Bakker, H. J. (2012). Complex formation in aqueous trimethylamine-N-oxide (TMAO) solutions. J Phys Chem B 116, 4783-4795.
45. Fielding, L. (2003). Nmr methods for the determination of protein-ligand dissociation constants. Curr Top Med Chem 3, 39-53.
46. Stirnemann, G., Duboue-Dijon, E., and Laage, D. (2017). Ab initio simulations of water dynamics in aqueous TMAO solutions: Temperature and concentration effects. J Phys Chem B 121, 11189-11197.
47. Niether, D., Di Lecce, S., Bresme, F., and Wiegand, S. (2018). Unravelling the hydrophobicity of urea in water using thermodiffusion: Implications for protein denaturation. Phys Chem Chem Phys 20, 1012-1020.
48. Trzesniak, D., Kunz, A. P. E., and van Gunsteren, W. F. (2007). A comparison of methods to compute the potential of mean force. ChemPhysChem 8, 162-169.

49. Ryckaert, J.-P., Ciccotti, G., and Berendsen, H. J. C. (1977). Numerical integration of the cartesian equations of motion of a system with constraints: Molecular dynamics of n-alkanes. J. Comput. Phys. 23, 327-341.
50. Duffy, E. M., Kowalczyk, P. J., and Jorgensen, W. L. (1993). Do denaturants interact with aromatic-hydrocarbons in water. J Am Chem Soc 115, 9271-9275.
51. Berendsen, H. J. C., Grigera, J. R., and Straatsma, T. P. (1987). The missing term in effective pair potentials. J Phys Chem 91, 6269-6271.
52. Bussi, G., Donadio, D., and Parrinello, M. (2007). Canonical sampling through velocity rescaling. J Chem Phys 126, 014101.
53. Hutter, J., Iannuzzi, M., Schiffmann, F., and VandeVondele, J. (2014). Cp2k: Atomistic simulations of condensed matter systems. Wiley Interdiscip Rev Comput Mol Sci 4, 15-25.
54. Lin, I. C., Seitsonen, A. P., Tavernelli, I., and Rothlisberger, U. (2012). Structure and dynamics of liquid water from ab initio molecular dynamics-comparison of BLYP, PBE, and revPBE density functionals with and without van der waals corrections. J Chem Theory Comput 8, 3902-3910.
55. Lin, I. C., Seitsonen, A. P., Coutinho-Neto, M. D., Tavernelli, I., and Rothlisberger, U. (2009). Importance of van der waals interactions in liquid water. J Phys Chem B 113, 1127-1131.
56. Galib, M., Duignan, T. T., Mistelib, Y., Baer, M. D., Schenter, G. K., Hutter, J., and Mundy, C. J. (2017). Mass density fluctuations in quantum and classical descriptions of liquid water J Chem Phys 146, 244501.
57. Goedecker, S., Teter, M., and Hutter, J. (1996). Separable dual-space gaussian pseudopotentials. Phys Rev B 54, 1703-1710.
58. Rezus, Y. L., and Bakker, H. J. (2006). Orientational dynamics of isotopically diluted H2O and D2O. J Chem Phys 125, 144512.
59. Beckonert, O., Keun, H. C., Ebbels, T. M., Bundy, J., Holmes, E., Lindon, J. C., and Nicholson, J. K. (2007). Metabolic profiling, metabolomic and metabonomic procedures for NMR spectroscopy of urine, plasma, serum and tissue extracts. Nat Protoc 2, 2692-2703.